

wall or the centreline of the casting, depending on the flow parameters [6]. The sedimentation of reinforcement particles due to gravity is a relevant concern both in the melt prior to casting and also in the solidifying casting if the time to solidification is of sufficient length [7,8]. The latter two factors are both strong functions of the particle/matrix density difference.

In the present work sedimentation experiments have been performed in order to compare the velocity of particle settling to the predicted Stokes' settling velocity for individual particles [9]. Previous studies using melt holding times of up to 90 minutes have reported significant sedimentation and it was proposed that clustering of the reinforcement particles was a possible mechanism for the excessively rapid settling rate observed [8]. The emphasis of the present work was to investigate the particle sedimentation, especially in the initial stages of settling. In addition, directional solidification experiments were conducted with Comral 90F composite and also with AA603 alloy in order to examine the influence of microspheres on the solidification of the matrix alloy and to study the behaviour of the microspheres during solidification.

Experimental procedure

Settling experiments

The sedimentation behaviour of Comral 90F composite was investigated using two sampling methods, tube-containment and ladling, in order to observe the effects of both settling time and volume fraction of reinforcement. The experiments were undertaken using an electric furnace with a bonded clay-graphite crucible. Both sets of samples were taken from the same melt which was held isothermally at 710 °C for the duration of the experiment. The melt was mechanically stirred for approximately three minutes to achieve initial homogeneity of particle distribution prior to each sampling.

Tube samples. Stainless steel tubes of length 250 mm and diameter 30 mm were immersed in the melt. The tubes were sealed at the base, but open at the top to allow filling. After the completion of filling, the tubes were held in an upright position in the melt, then removed and water-quenched at successively increasing holding times ranging from 0 to 20 minutes. Sampling in this manner ensured that all tubes had the same volume fraction of reinforcement particles, and thus allowed the sedimentation to be characterised in terms of the height of the particle-free zone formed at the top of the sample as a function of holding, or settling, time.

Ladled samples. In these experiments the melt was allowed to settle and was sampled at increasingly long holding times. A hemispherical steel ladle was used to take a sample from the upper region of the melt. The material in the ladle was manually stirred with a stainless steel paddle to achieve homogeneity, then poured into a steel mould of diameter 40 mm and immediately quenched in water. Due to settling of the melt in the crucible, the volume fraction of reinforcement particles in the upper region decreased with increasing holding time, and hence the samples ladled from this region had decreasing volume fractions of reinforcement. This process allowed the settling behaviour of composite material with different volume fractions of reinforcement to be studied. The

time period available for settling processes within the steel mould was \approx 20 seconds, corresponding to the time to complete solidification.

Directional solidification experiments

Molten Comral 90F composite was drawn into alumina tubes of inner diameter 4 mm, outer diameter 6 mm and length 500 mm for directional solidification in a vertical Bridgeman type furnace. Two furnace travel rates, 15 and 100 μms^{-1} , were used in the experiment. For comparison with the composite, AA603 alloy was also studied in directional solidification under the same conditions as those for Comral 90F composite. The AA603 Al alloy was extracted from the Comral 90F composite by allowing the molten MMC to settle for a sufficiently long time (typically 30 minutes) so that the matrix alloy could be obtained from the surface region of the melt containing no microspheres. Quantitative metallography for the characterisation of particle distribution and particulate volume fraction was carried out with a Cambridge Instruments Quantimet 570 image analyser.

Results and discussion

Sedimentation

The sedimentation height (a dimensionless ratio of the height of the sedimented region to the total sample height) was measured for each tube sample and plotted as a function of the settling time (Fig. 1). It is evident that the sedimentation rate had decreased substantially after the initial 10 minutes of isothermal settling. The results suggest that the rate decreases as the maximum packing density of ceramic spheres is approached. Previous studies [8] have found that at holding times longer than 20 minutes the settled region would have reached the maximum packing density of particulate, and no further appreciable settling would have occurred. The average settling velocity during the first 10 minutes was approximately 0.15 mms^{-1} , which is about an order of magnitude higher than the predicted Stokes settling velocity for individual particles. The demarcation between the particle-free zone and sedimented region was always very sharp, as shown in a typical axial view of a tube sample (Fig. 2).

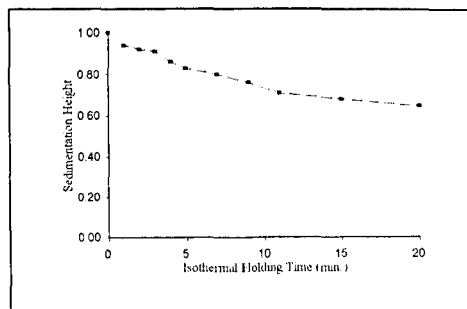


Figure 1. Sedimentation height plotted as a function of holding time for tube samples.

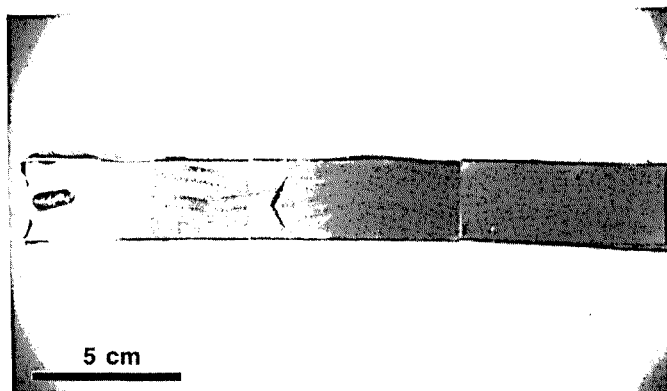


Figure 2. Axial cross-section of a tube sample which was held isothermally for 4 minutes. The particle-free zone is in light contrast at left.

The ladled samples were sectioned and polished for metallographic study using image analysis techniques. The volume fraction of reinforcement for each sample was determined by averaging the area fraction measurements of 25 contiguous fields at the edge of the casting. The edge region corresponds to the chill zone, which would best represent the initial concentration of particles prior to any settling which may occur during solidification. Thermocouple readings taken from trial castings showed that this edge region of the samples solidified within 1 second, and the time to solidification in the central region was approximately 20 seconds. These samples therefore allowed the settling behaviour of the composite with various volume fractions of reinforcement to be observed over settling time periods ranging from less than a second to about 20 seconds.

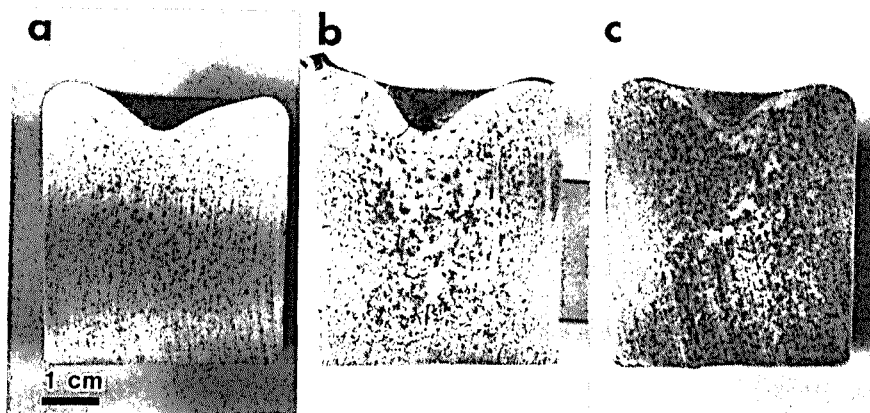


Figure 3. Cross-sections of ladled samples with different volume fractions of reinforcement: (a) low; (b) intermediate; and (c) high. Microsphere-rich areas are in dark contrast.

Three distinctly different settling behaviours were observed, corresponding to different volume fraction regimes of reinforcement (Fig. 3). Samples having a low volume fraction of reinforcement ($\leq 2\%$) had quite a small particle-free zone at the top and the size of this zone decreased with decreasing volume fraction. Small clusters of particles were observed throughout the casting. The size of the particle-free zone allowed comparison of the settling rate between samples to be made directly, since the settling time (corresponding to the solidification time) for a particular region considered was similar for each sample. The small particle-free zone was thus indicative of a low settling rate. Intermediate volume fraction samples ($2\% \leq V_f \leq 10\%$) exhibited a very large particle free zone at the top, indicating a high rate of settling (Fig. 3(b)). Large agglomerates of particles were present, especially in the central region of the castings. Samples of high volume fraction of reinforcement particles (10 to 20 %) tended to have a smaller particle-free zone at the top than those of intermediate volume fraction, and the zone narrowed further as the volume fraction became quite high (Fig. 3(c)). This was likewise interpreted as a decrease in settling rate as the volume fraction increased. The distribution of particles suggests that a particle skeleton had formed, with most particles in contact with near neighbours.

The above observations suggest that settling proceeds at low rates for samples having a low volume fraction of reinforcement, corresponding to the sedimentation of single particles or fine clusters, until the volume fraction reaches levels that allow the easy formation of large clusters (agglomerates). These agglomerates settle as one particle, thus the sedimentation rate is high, as observed in samples of intermediate volume fraction. At still higher volume fractions, the agglomerates become close enough to form a network (or solid skeleton), after which further sedimentation must occur by the packing and rearrangement of particles until maximum packing density is reached. Packing is a slower process than the settling of clusters, as the particles are already in contact with others and must dissociate and rearrange in order to achieve a higher spatial density.

Directional solidification

Eutectic Si. For the range of furnace travel rates used (15 and 100 μms^{-1}), the effect of cooling rate on the morphology of eutectic Si seemed negligible for the AA603 alloy as shown in Figs. 4 (a) and (c). However, in samples of Comral 90F composite the eutectic Si in specimens where the furnace travel rate was 15 μms^{-1} appeared not only much coarser than in those of 100 μms^{-1} , but also angular and blocky in shape (Figs. (b) and (d)). This morphological change in the Comral 90F composite could possibly be related to an increase in temperature gradient along the specimen tube because of the poor thermal conductivity of the ceramic spheres. When the ratio of the temperature gradient to the growth velocity is high, the growth of the two phases in a eutectic tends to be independent and, consequently, coarse microstructures are formed.

Al dendrites. Directional solidification at both furnace travel rates produced a dendritic morphology for the Al phase in AA603. However, because of the presence of the microspheres, the Al phase in Comral 90F composite appeared columnar (i.e., cells elongated along the growth direction) when the furnace travel rate was 15 μms^{-1} (Fig. 5). The spheres seem to have been pushed by the advancing growth front of Al such that lines and pockets of microspheres could be seen between the columnar Al cells. The

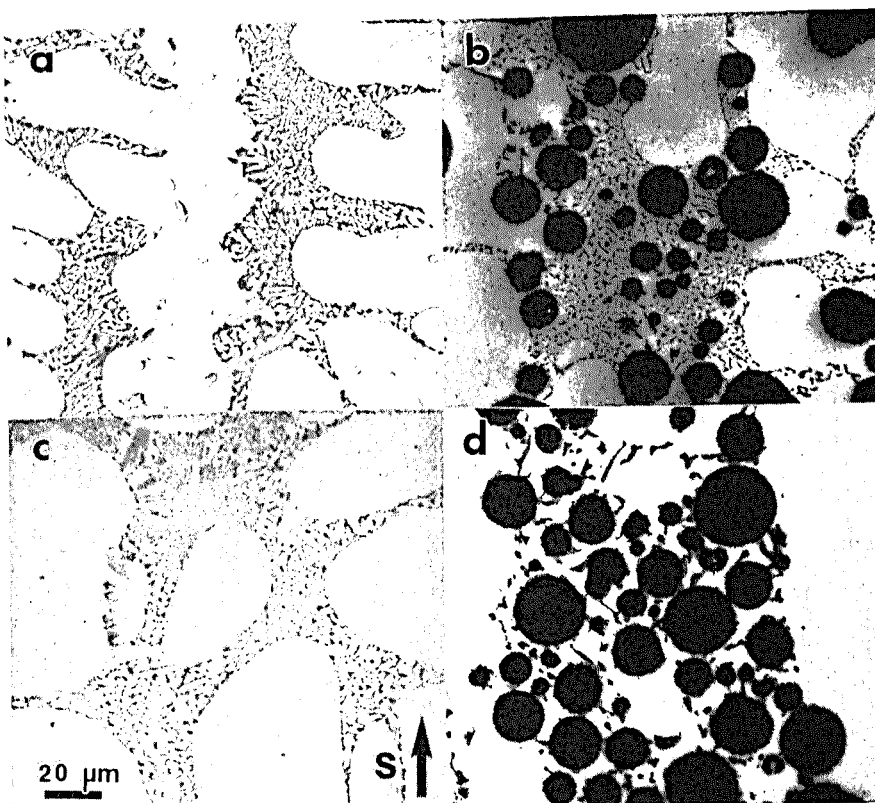


Figure 4. Optical micrographs of directionally solidified specimens: (a) AA603, $100 \mu\text{m s}^{-1}$; (b) Comral 90F composite, $100 \mu\text{m s}^{-1}$; (c) AA603, $15 \mu\text{m s}^{-1}$; and (d) Comral 90F composite, $15 \mu\text{m s}^{-1}$. The arrow indicates the direction of solidification.

morphology of the Al phase changed from elongated cellular to a more typically rounded cellular shape and lost directionality when the rate of travel of the furnace was increased from $15 \mu\text{m s}^{-1}$ to $100 \mu\text{m s}^{-1}$ (Fig. 6). It appeared that the presence of microspheres altered the local temperature gradient during directional solidification because of their poor thermal conductivity, and thus at this increased furnace travel rate the solidification front advanced in different directions. It can be seen that the average cross-section of Al dendrite arms (cell size) of the Al phase, was similar to that of the microspheres (Fig. 6). The spheres seemed to have been pushed by the solidification front for a distance similar to the cell size, but in various directions. This is in contrast to the case of the $15 \mu\text{m s}^{-1}$ travel rate (Fig. 5(b)), where the growth of Al was directional and consequently the microspheres were pushed laterally into the intercellular regions. It is obvious that the distribution of microspheres in the specimen produced at a furnace travel rate of $100 \mu\text{m s}^{-1}$ appears to be more uniform than that of the $15 \mu\text{m s}^{-1}$ specimen. This observation indicates that the uniformity of microspheres in the specimen can be improved by controlling the cooling rate and temperature gradient.

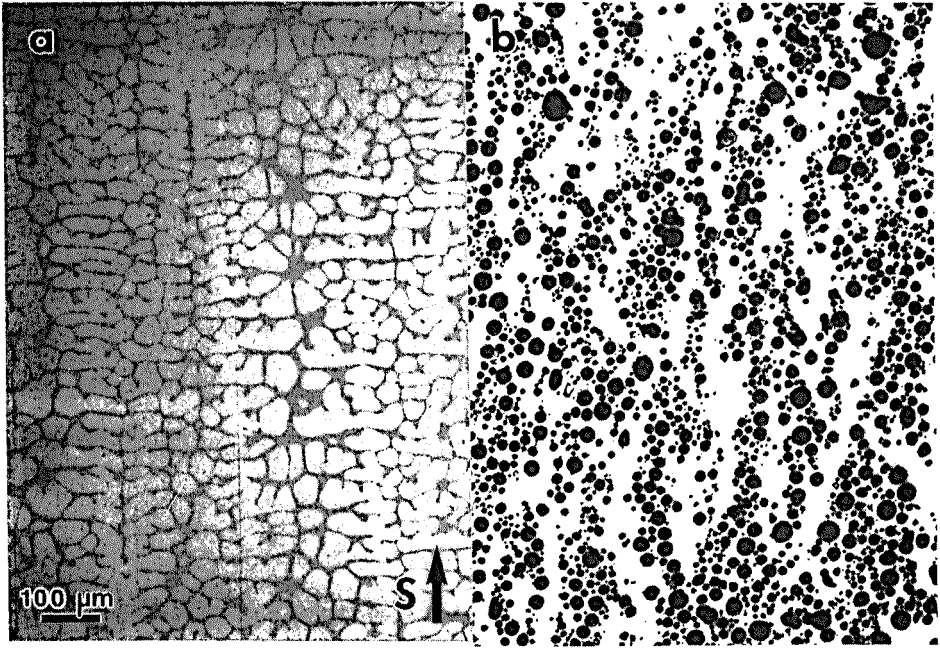


Figure 5. Optical micrographs of directionally solidified specimens of (a) an AA603 alloy, and (b) Comral 90F composite at furnace travel rate $15 \mu\text{m}\cdot\text{s}^{-1}$.

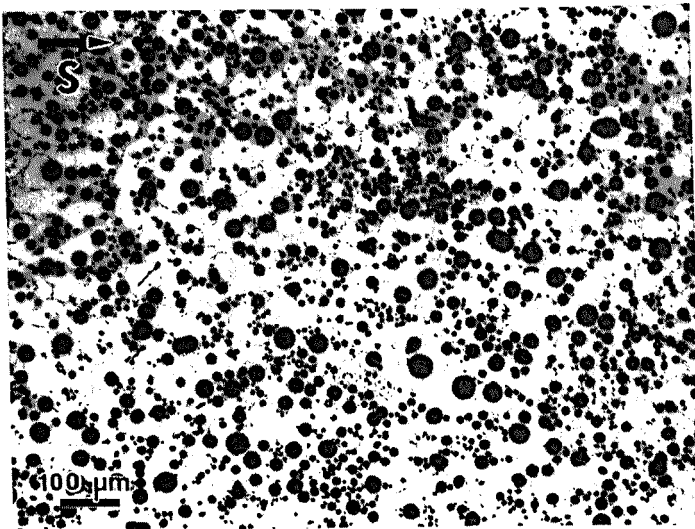


Figure 6. Optical micrograph of a directionally solidified specimen of Comral 90F composite at a furnace travel rate of $\approx 100 \mu\text{m}\cdot\text{s}^{-1}$.

Conclusion

It was found that sedimentation of reinforcement particles in the melt occurred rapidly over short time-scales, and could not be attributed simply to the sedimentation of individual particles according to Stokes' theory. Settling behaviour can be characterised with respect to the volume fraction of particulate in the sample, with three different modes of behaviour observed. Fast settling occurred in melts with mid-range particle volume fractions, and could be attributed to the observed formation of agglomerates of microspheres which are assumed to settle as one particle. Settling in melts of low and high volume fraction of particles was slow. At low volume fractions the particles settled as individual microspheres or in small clusters. At high volume fractions, agglomerates in a skeletal structure underwent a slower process of packing and rearrangement.

The solidification of Al in Comral 90F composite was significantly influenced by the presence of ceramic microspheres. At a furnace travel rate of $15 \mu\text{ms}^{-1}$, the Al phase in AA603 was dendritic, while it was columnar in Comral 90F composite. Furthermore, the presence of microspheres seemed to reduce the local cooling rate such that the eutectic Si crystals were finer in AA603 than in Comral 90F composite. A relatively uniform distribution of the microspheres was obtained with a high imposed solidification rate ($100 \mu\text{ms}^{-1}$).

Acknowledgements

This work has been supported by grants from the Australian Industrial Research and Development Board (IRDB 15053), Comalco Aluminium Limited and PBR Automotive Pty Ltd and also from the CRC for Alloy and Solidification Technology (CAST). Discussions with Drs M. Couper, W. Thorpe, L. Hogan, and Professor G. Dunlop are gratefully acknowledged.

References

1. M.J. Couper and K. Xia, Proc. 12th Risø International Symposium on Materials Science, Roskilde, Denmark (1991).
2. J.Y. Yao, G.A. Edwards, M.J. Couper and G.L. Dunlop, Proc. Interface II, Ballarat, Victoria, Australia (1993).
3. A. Kolsgaard, L. Arnberg and S. Brusethaug, *Mat. Sci. Eng.*, **A173**, (1993), 243.
4. D.R. Uhlmann, B. Chalmers and K.A. Jackson, *J. App. Phys.*, **35**, (1964), 2986.
5. A.R. Kennedy and T.W. Clyne, *Cast Metals*, **4**, (1991), 160.
6. Q. Han and J.D. Hunt, *Mat. Sci. Eng.*, **A173**, (1993), 221.
7. G.S. Hanumanth, G.A. Irons and S. Lafreniere, *Metall. Trans. B*, **23B**, (1992), 753.
8. N. Setargew, B.A. Parker and M.J. Couper, Proc. Advanced Composites '93, Wollongong, Australia (1993).
9. J.F. Richardson and W.N. Zaki, *Trans. Instn Chem. Engrs*, **32**, (1954), 35.